<Original Paper>
Journal of the Korean Society for Nondestructive Testing, Vol. 37, No. 2: 75-83, 2017
ISSN 1225-7842 / eISSN 2287-402X http://dx.doi.org/10.7779/JKSNT.2017.37.2.75

Thermal Analysis of Silicon Carbide Coating on a Nickel based Superalloy Substrate and Thickness Measurement of Top Layers by Lock-in Infrared Thermography

Shrestha Ranjit* and Wontae Kim**†

Abstract In this paper, we investigate the capacity of the lock-in infrared thermography technique for the evaluation of non-uniform top layers of a silicon carbide coating with a nickel based superalloy sample. The method utilized a multilayer heat transfer model to analyze the surface temperature response. The modelling of the sample was done in ANSYS. The sample consists of three layers, namely, the metal substrate, bond coat and top coat. A sinusoidal heating at different excitation frequencies was imposed upon the top layer of the sample according to the experimental procedures. The thermal response of the excited surface was recorded, and the phase angle image was computed by Fourier transform using the image processing software, MATLAB and Thermofit Pro. The correlation between the coating thickness and phase angle was established for each excitation frequency. The most appropriate excitation frequency was found to be 0.05 Hz. The method demonstrated potential in the evaluation of coating thickness and it was successfully applied to measure the non-uniform top layers ranging from 0.05 mm to 1 mm with an accuracy of 0.000002 mm to 0.045 mm.

Keywords: Silicon Carbide Coating, Nickel Based Superalloy, Thickness Measurement, Lock-In Thermography, Phase Angle

1. Introduction

Coating technology is widely used in modern industries and applications to prolong the life of components [1,2]. Silicon carbide (SiC) has the properties of hot temperature oxidation resistance, stability against hot corrosion and good thermal shock [3-5]. Hence, SiC ceramic coating provides the combined mechanical and physicochemical properties such as extreme hardness, high strength, resistance to oxidation, corrosion and wear [6]. Ceramic coated components are steadily increasing its importance in aircraft, power generation and automotive industries due to excellent thermal insulation. In the automotive industry, it has effects on the fatigue life of the engine components, fuel consumption, power & combustion efficiency and pollution contents. Meanwhile, in the aerospace industry, it is used as a thermal barrier coating to protect turbine engine components in hot temperature or hostile environments [7-9]. Because of the stringent safety requirements in these industries, quality control of these products is an essential part of their fabrication. Therefore, determination of coating thicknesses is of paramount importance in defining their performance and properties. However, the nature of coatings is so diverse that there can be no single technique that fully characterizes them. Thus, the effectiveness of non-destructive testing (NDT) for the evaluation of coating is of great significance. Infrared thermography (IRT) as a NDT can be used for the testing and evaluation of coating [10-18]. IRT deals with the acquisition and analysis of thermal data from non-contact thermal imaging

[Received: February 10, 2017, Revised: April 18, 2017, Accepted: April 25, 2017] *Dept. of Mechanical Engineering, Graduate School, Kongju National University, Cheonan 31080, Rep. of Korea, **Div. of Mechanical & Automotive Engineering, Kongju National University, Cheonan 31080, Rep. of Korea, † Corresponding Author: kwt@kongju.ac.kr

devices based on that all bodies emit infrared energy with the absolute temperature above 0 K. IRT has been used in the inspection of physical and mechanical properties, discontinuities, sub-surface defects and features, hidden corrosion and coating thickness. IRT being NDT approach involves two classes, passive thermography and active thermography. Based on the heating methods, active thermography could be further classified into pulsed thermography (PT), lock-in thermography (LIT), pulsed phase thermography (PPT), step heating (ST), Vibrothermography (VT). In the active approach of NDT, PT and LIT are the most commonly used approaches. In LIT, a sinusoidal heat flux is used to excite the sample and the amplitude and phase images can be obtained by reconstructing the surface wave signal using appropriate algorithms [19-23].

LIT is found effective for the evaluation of coating thickness because it detects the thermal information which depends on the thermal properties of the test sample under consideration. When a test sample is excited by a thermal energy then the system utilizes an infrared camera to observe the surface temperature of a thermal wave propagating into the sample material. The heat transfer from the sample surface is affected by internal material structures and properties. Therefore, by developing appropriate data processing methods, pertinent coating parameters may be derived from the thermal data. Thermal data are sensitive to several important coating parameters such as thermal conductivity, specific heat capacity and the thickness of the top ceramic layer [24-27].

This paper presents the finite element analysis (FEA) based study of LIT technique for the evaluation of SiC ceramic coating deposited on nickel base super alloys. FEA software, ANSYS was used for the modelling of the sample. A reference sample with known and non-uniform top layers ranging from 0.025 mm to 1 mm, was used in the study. A variety of coating layers were chosen to illustrate the effects of thickness on the observed thermal response. The top layer of the coating was excited by a calculated thermal energy to predict the surface temperature distribution on the sample. The analysis was performed at several excitation frequencies beginning from 0.2 Hz down to 0.01 Hz. Image processing softwares, MATLAB and Thermofit Pro were used to extract the phase angle image from thermal sequences using a Fourier transform. The correlation of coating thickness and phase angle was established and the thickness of top layers was predicted.

2. Materials and methods

2.1. Lock-in infrared thermography (LIT)

LIT is a technique derived from photo thermal radiometry in which the sample is exposed to sinusoidal temperature stimulation. LIT in reflection mode was considered in this study. Fig. 1 shows the schematic of experimental LIT. AS shown in Fig. 1, IR camera and the excitation source are positioned facing the same surface of the test sample. When the excitation source is imposed on the sample, it absorbs some incident energy and produces a localized heat flow following a non-radiative process. The modulated excitation source produced a periodic heat flow which is a diffusive process

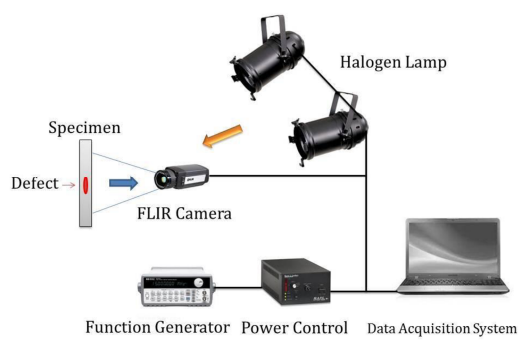

Fig. 1 Schematic of experimental Lock-in thermography

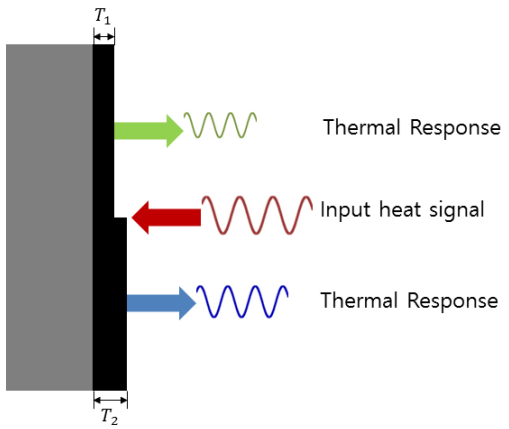

Fig. 2 Theory of Lock-in thermography for the evaluation of coating thickness

resulting a periodic temperature distribution called a thermal wave. Hence, the thermal response of the inspected object's is also a sinusoidal wave as shown in Fig. 2, whose amplitude and phase depends on the input sinusoidal temperature stimulation and the object's material. The phase of the temperature change varies due to different thermal wave propagation distance when the coating thickness changes [28-30].

The front surface of the coating sample is subjected to plane harmonic heat and thermal excitation formed is expressed as Eq. (1) [20,31,32],

$$q(t) = \frac{q_0}{2}(1 + \cos(2\pi f t)) \quad (1)$$

where $q(t)$ is the instantaneous density of the sinusoidal heat flux, q_0 is the heating power of the heat source, f is the excitation loading frequency of the heat source.

Heat propagates through the coating sample by heat conduction and the resulting temperature T(t,z) attenuates exponentially with thickness z, as expressed by Eq. (2) [19-21,32],

$$T_{z,t} = A(z)\cos[\omega t - \emptyset(z)] = T_0 e^{-\frac{z}{\mu}} \cos\left(2\pi f t - \frac{2\pi z}{\lambda}\right) \quad (2)$$

where, T_0 [°C] is initial change in temperature by a heat source, z [mm] is the coating thickness, ω [rad/s] is the modulation frequency, f [Hz] is the frequency, λ [m] is thermal wavelength, A (z) is the thermal amplitude, $\phi(z)$ is the phase, and μ [m] is thermal diffusion length defined by Eq. (3),

$$\mu = \sqrt{\frac{\alpha}{\pi f}} \quad (3)$$

where, $\alpha = \frac{k}{\rho . c_p}$ [m^2s^{-1}] is the material thermal diffusivity with k [W/m°C] being thermal conductivity, ρ [kg/m^3] the density and C_p [J/kg°C] the specific heat.

The Fourier transform is used to extract phase angle from the thermal sequences. The Fourier transform is expressed as Eq. (4) [33,34],

$$F_n = \Delta t \sum_{k=0}^{N-1} T(k\Delta t) \exp^{\frac{j2\pi nk}{N}} = Re_n + Im_n \quad (4)$$

Real and imaginary parts of the complex transform are used to estimate the phase angle and expressed as Eq. (5),

$$\emptyset_n = \tan^{-1}\left(\frac{Im_n}{Re_n}\right) \quad (5)$$

2.2. Finite Element Modelling (FEM)

A 3-D heat flow model was created in "ANSYS' to simulate the LIT inspection. Fig. 3 shows the schematic description of coating layers with substrate material. As shown in Fig. 3, the predominant material, silicon carbide, is used as the top coat and the intermetallic material, MCrAIY is used as a bond coat on the nickel based super alloy substrate. The substrate and the bond coat thickness were kept at 4 mm and 0.1 mm, respectively. Whereas the top coating thickness was varied from 0.025 mm to 1 mm.

Fig. 4 shows the geometrical details of the test sample. Fig. 5 shows the FEA model of the sample. A meshing of the sample was adapted

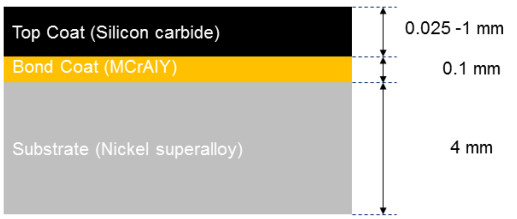

Fig. 3 Schematic description of coating layers with substrate material

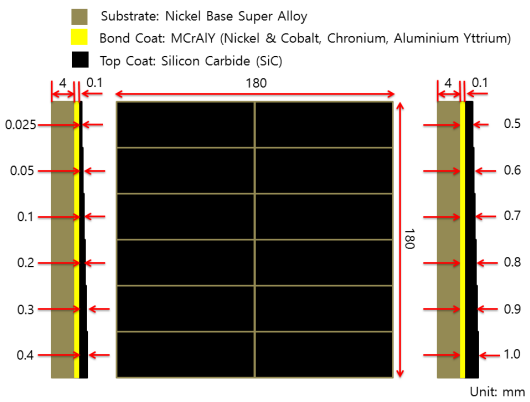

Fig. 4 Geometrical details of the sample

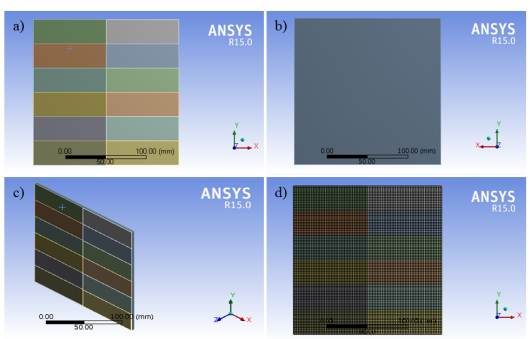

Fig. 5 FEA model of the sample, (a) front surface, (b) back surface, (c) 3-D model and (d) model with meshing

Table 1 Thermo-mechanical properties of coating layers

Layers	Density (kg/m^3)	Conductivity (W/mk)	Heat capacity (J/kg.K)
Top coat	3210	120	670
Bond coat	3984	3.3	755
Substrate	8440	9.92	410

to calculate temperature variations with sufficient spatial resolution. The resulting mesh had 162,000 elements and 854,685 nodes. The physical preference was considered as mechanical with relevance 100, relative center was kept in fine mode and proximity and curvature were kept on in advanced size function. Table 1 shows the thermo-mechanical properties of coating layers considered in the analysis [1,35].

During simulation, 2 kW intensity of heat resource was considered. The time-step was determined by the excitation frequency and analysis periods were set to $\frac{2}{100^* f}$, where f is the excitation frequency. The simulation was done at different excitation frequencies ranging from 0.2 Hz down to 0.01 Hz.

3. Results and discussions

The response of the applied heat flux was simulated for 20 complete excitation cycles at frequencies 0.2 Hz, 0.1 Hz, 0.05 Hz, 0.02 Hz and 0.01 Hz, respectively. The surface temperature of the sample evolved periodically in a sinusoidal pattern from the transient state to the steady state. Fig. 6 shows the surface temperature evolution of 0.2 mm thick coating at 0.2 Hz frequency. As can be seen in Fig. 6, it took almost 12 periodic cycles to reach the steady state from the transient state.

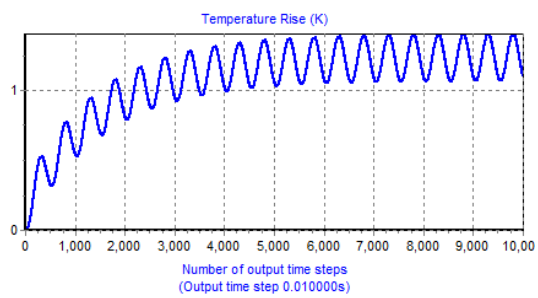

Fig. 6 Simulated surface temperature evolution of 0.2 mm coating at the excitation frequency of 0.2 Hz

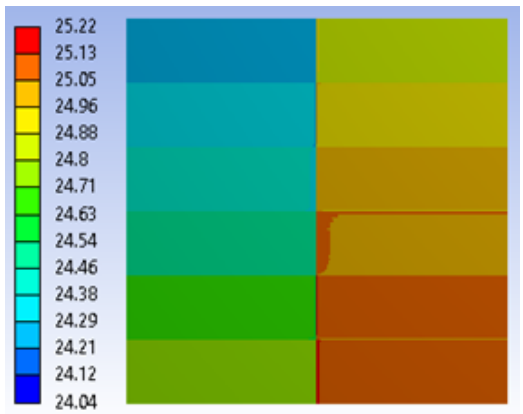

(a) 1st cycle, time 0.8 s

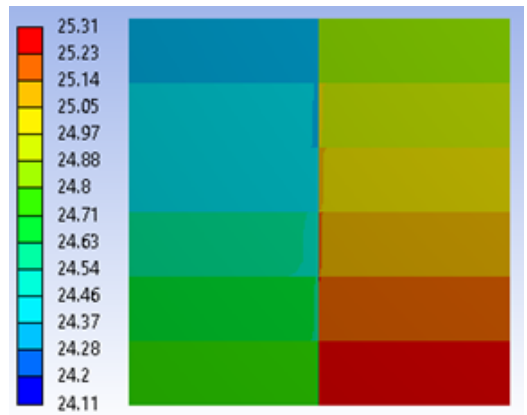

(b) 1st cycle, time 2 s

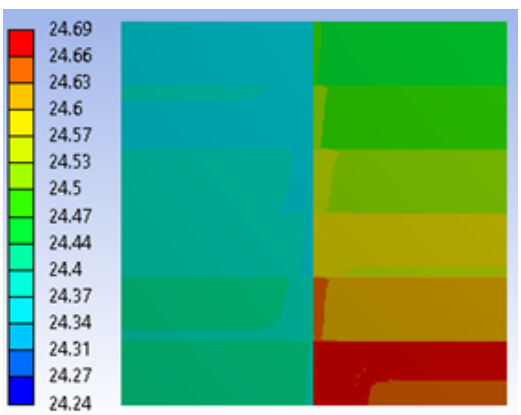

(c) 1st cycle, time 3 s

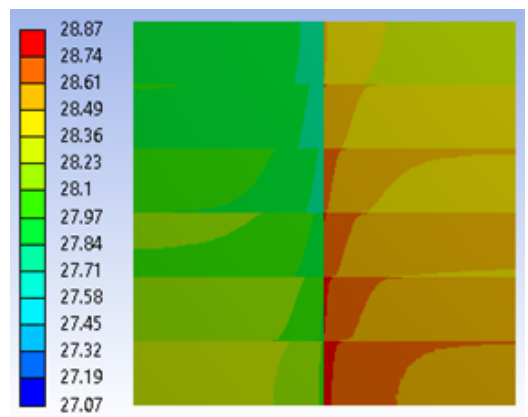

(d) 12th cycle, time 61 s

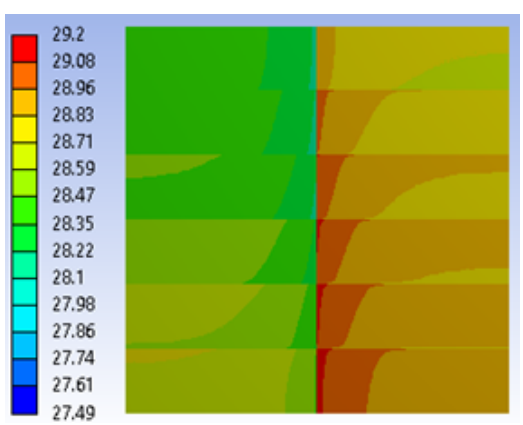

(e) 12th cycle, time 62 s

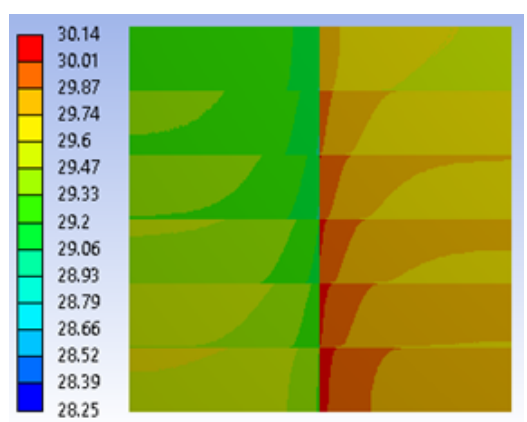

(f) 12th cycle, time 63 s

Fig. 7 Simulated Lock-in thermal images at different excitation cycle with time for 0.2 Hz frequency.

Fig. 7 shows the lock-in thermal images of coatings with different thickness at different excitation cycles for 0.2 Hz frequency. As can be seen in Fig. 7, thick coating attained a maximum temperature when compared wth thin coating.

Fourier transform was used to compute the phase angle image for all the excitation frequencies. The pre-processing of thermal images was done in MATLAB and Fourier transform was performed in ThermoFit Pro. Then the plotting of phase angle and coating thickness as a function of excitation frequencies was done. Fig. 8 shows the phase image at excitation frequency 0.2 Hz. Fig. 9 shows the plot of coating thickness and phase angle as a function of excitation frequencies. As can be seen in Fig. 8 and Fig. 9, phase angle increased with the increasing coating thickness and decreased with the decreasing frequency.

The 6th order polynomial fitting was adopted to correlate the coating thickness and phase angle for all the excitation frequencies. The best correlation between the coating thickness and phase angle was found at the frequency 0.05 Hz with R-square(R^2) = 0.99619 and adj. R-square(aR^2) = 0.99048. So, the phase image at 0.05 Hz frequency was considered for the further analysis and the correlation between the coating thickness and phase angle is expressed as Eq. (6).

$$T = -18.32 - 53.32\phi + 18.84\phi^2 - 64.50\phi^3 - 54.85\phi^4 + 16.04\phi^5 - 1.63\phi^6 \quad (6)$$

Eq. (6) was used to predict the thickness of the coatings. Then predicted thickness was compared with the actual thickness and the percentage error was calculated. Table 2 shows the details of phase angle, predicted thickness and the percentage error. As can be seen in Table 2, the percentage error involved in measurement is within the acceptable limit.

Fig. 8 Phase image acquired with the Fourier transform at the excitation frequency of 0.2 Hz

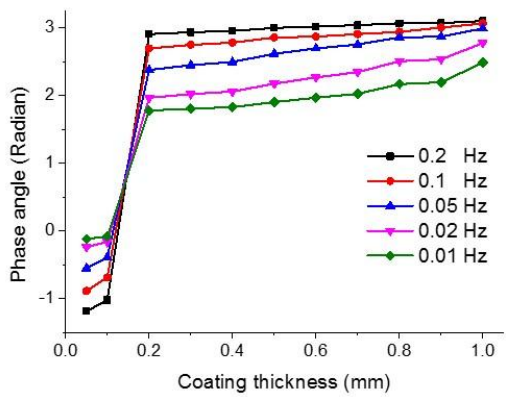

Fig. 9 Coating thickness and phase angle as a function of excitation frequencies

Table 2 Predicted coating thickness and percentage error

Actual thickness (mm)	Calculated Phase angle (radian)	Predicted thickness (mm)	Percentage error (%)
0.05	-0.552	0.050	0.004
0.1	-0.390	0.100	0.002
0.2	2.378	0.198	0.843
0.3	2.446	0.318	5.944
0.4	2.494	0.381	4.716
0.5	2.617	0.514	2.881
0.6	2.694	0.605	0.882
0.7	2.752	0.686	2.058
0.8	2.854	0.845	5.663
0.9	2.870	0.870	3.295
1.0	2.989	1.005	0.502

4. Conclusions

This study explored the use of LIT inspection process for the evaluation of non-uniform coating thickness. FEA software, 'ANSYS Ver. 15' was used to simulate the LIT inspection process. Image processing softwares, 'MATLAB' was used for the pre-processing of thermal images and 'Thermofit Pro' was used to compute the phase angle image using Fourier transform. The differences in the temperature of thermal image and its corresponding phase angle played the significant role in the evaluation of coating thickness. In addition, it is also found that correct excitation frequency must be selected for the accurate evaluation of coating thickness. The method demonstrated potential in the evaluation of coating thickness and was successfully applied to measure the non-uniform coating thickness ranging from 0.05 mm to 1 mm within an accuracy of 0.000002 mm to 0.045 mm. The estimated coating thickness was found in good agreement with the actual value.

Acknowledgement

This work was supported by the National Research Foundation of Korea (NRF) grant funded by the Ministry of Education, Science and Technology (NRF-2014R1 A1A2054595) and (NRF-2016R1D1A1B03932587).

References

[1] S. Ranjit, Y. Chung and W. Kim, "Thermal behavior variations in coating thickness using pulse phase thermography," *Journal of the Korean Society for Nondestructive Testing*, Vol. 36, No. 4, pp. 259-265 (2016)

[2] S. Mezghani, E. Perrin, V. Vrabie, J. Bodnar, J. Marthe and B. Cauwe, "Evaluation of paint coating thickness variations based on pulsed Infrared thermography laser technique," *Infrared Physics & Technology*, Vol. 76, pp. 393-401 (2016)

[3] J. Roy, S. Chandra, S. Das and S. Maitra, "Oxidation behaviour of silicon carbide-a review," *Rev. Adv. Mater. Sci*, Vol. 38, pp. 29-39 (2014)

[4] R. Munro and S. Dapkunas, "Corrosion characteristics of silicon carbide and silicon nitride," *Journal of research of the National Institute of Standards and Technology*, Vol. 98, No. 5, pp. 607 (1993)

[5] X. Yang, C. Zhao-hui and C. Feng, "High-temperature protective coatings for C/SiC composites," *Journal of Asian Ceramic Societies*, Vol. 2, No. 4, pp. 305-309 (2014)

[6] R. Venugopalan, "Development of carbon based materials with SiC coating for high temperature nuclear applications," *Doctoral Dissertation*, Homi Bhabha National Institute, (2012)

[7] H. Crostack, W. Jahnel, E. Meyer and K. Pohl, "Recent developments in non-destructive testing of coated components," *Thin Solid Films*, Vol. 181, No. 1-2, pp. 295-304 (1989)

[8] K. R. Sharma and G. Kumar, "Thermo-mechanical experiments of Y-PSZ thermal barrier ceramic coating with bond coat of alumina," *Journal of The Institution of Engineers (India): Series C*, Vol. 96, No. 3, pp. 287-298 (2015)

[9] D. J. Roth, L. M. Cosgriff, B. Harder, D. Zhu and R. E. Martin, "Absolute thickness measurements on coatings without prior knowledge of material properties using terahertz energy," *NASA Technical Reports*, NASA/TM 2013-216603, (2013)

[10] D. Wu, J. Rantala, W. Karpen, G. Zenzinger, B. Schönbach, W. Rippel, R. Steegmüller, L. Diener and G. Busse, "Applications of lockin-thermography methods," *Review of Progress in Quantitative Nondestructive Evaluation,* pp. 511-518 (1996)

[11] H. Wang, S. Hsieh, B. Peng and X. Zhou, "Non-metallic coating thickness prediction using artificial neural network and support vector machine with time resolved thermography," *Infrared Physics & Technology*, Vol. 77, pp. 316-324 (2016)

[12] J. Sun, N. Tao, D. E. Chimenti and L. J. Bond, "Thermal property measurement for thermal barrier coatings using pulsed thermal imaging-multilayer analysis method," *AIP Conference Proceedings*, AIP Publishing, Vol. 1706, No. 1, pp. 100004 (2016)

[13] J. Liu, Q. Tang, Y. Wang, J. Gong and L. Qin, "Investigation on coating uniformity of high-temperature alloy with SiC thermal barrier coating using pulsed infrared thermographic technique," *International Journal of Thermophysics*, Vol. 36, No. 5-6, pp. 1252-1258 (2015)

[14] M. Aoyagi, T. Hiraguri and T. Ueno, "Nondestructive analysis of uneven paint coatings by dynamic heat conduction following flash heating," *Journal of Coatings Technology and Research*, Vol. 11, No. 3, pp. 311-318 (2014)

[15] W. A. Ellingson, R. J. Visher, R. S. Lipanovich and C. M. Deemer, "Optical NDE methods for ceramic thermal barrier coatings," *Materials Evaluation*, Vol. 64, No. 1, pp. 45-51 (2006)

[16] J. Sun, "Pulsed thermal imaging measurement of thermal properties for thermal barrier coatings based on a multilayer heat transfer model," *Journal of Heat Transfer*, Vol. 136, No. 8, pp. 081601 (2014)

[17] O. Altun, Y. E. Boke and A. Kalemtas, "Problems for determining the thermal conductivity of TBCs by laser-flash method," *Journal of Achievements in materials and manufacturing engineering*, Vol. 30, No. 2, pp. 115-120 (2008)

[18] S. Marinetti, D. Robba, F. Cernuschi, P. Bison and E. Grinzato, "Thermographic inspection of TBC coated gas turbine blades: Discrimination between coating over-thicknesses and adhesion defects," *Infrared Physics & Technology*, Vol. 49, No. 3, pp. 281-285 (2007)

[19] R. Shrestha, J. Park and W. Kim, "Application of thermal wave imaging and phase shifting method for defect detection in Stainless steel," *Infrared Physics & Technology*, Vol. 76, pp. 676-683 (2016)

[20] S. Ranjit, K. Kang and W. Kim, "Investigation of lock-in infrared thermography for evaluation of subsurface defects size and depth," *International Journal of Precision Engineering and Manufacturing*, Vol. 16, No. 11, pp. 2255-2264 (2015)

[21] S. Ranjit, M. Choi and W. Kim, "Quantification of defects depth in glass fiber reinforced plastic plate by infrared lock-in thermography," *Journal of Mechanical Science and Technology*, Vol. 30, No. 3, pp. 1111-1118 (2016)

[22] Q. Tang, J. Liu, J. Dai and Z. Yu, "Theoretical and experimental study on thermal barrier coating (TBC) uneven thickness detection using pulsed infrared thermography technology," *Applied Thermal Engineering*, Vol. 114, pp. 770-775 (2017)

[23] S. Ranjit and W. T. Kim, "Detection of subsurface defects in metal materials using infrared thermography; image processing and finite element modeling," *Journal of the Korean Society for Nondestructive Testing*, Vol. 34, No. 2, pp. 128-134 (2014)

[24] J. Sun, "Development of Nondestructive Evaluation Methods for Thermal Barrier Coatings," *Proceedings of 22nd Annual Conf. on Fossil Energy Materials*, Pittsburgh, PA (2008)

[25] J. Zhang, X. Meng and Y. Ma, "A new measurement method of coatings thickness based on lock-in thermography," *Infrared*

Physics & Technology, Vol. 76, pp. 655-660 (2016)

[26] B. Venkatraman, M. Menaka, R. Subbaratnam and B. Raj, "Characterisation of colmonoy coatings using lock-in thermography," *17th World Conf. on Non-destructive Testing*, Shanghai, China (2008)

[27] X. Maldague, "Theory and practice of infrared technology for nondestructive testing," Wiley series microwave and optical engineering, pp. 355-363 (2001)

[28] X. P. Maldague and P. O. Moore, "Nondestructive testing handbook, Vol. 3: Infrared and thermal testing," *American Society for Nondestructive Testing*, (2001)

[29] V. Vavilov, "Infrared techniques for materials analysis and nondestructive testing," *Infrared methodology and technology*, pp. 230-309 (1994)

[30] Y. Duan, S. Huebner, U. Hassler, A. Osman, C. Ibarra-Castanedo and X. P. Maldague, "Quantitative evaluation of optical lock-in and pulsed thermography for aluminum foam material," *Infrared Physics & Technology*, Vol. 60, pp. 275-280 (2013)

[31] J. Liu, W. Yang and J. Dai, "Research on thermal wave processing of lock-in thermography based on analyzing image sequences for NDT," *Infrared Physics & Technology*, Vol. 53, No. 5, pp. 348-357 (2010)

[32] C. Meola and G. M. Carlomagno, "Recent advances in the use of infrared thermography," *Measurement science and technology*, Vol. 15, No. 9, pp. R27 (2004)

[33] X. Maldague and S. Marinetti, "Pulse phase infrared thermography," *Journal of Applied Physics*, Vol. 79, No. 5, pp. 2694-2698 (1996)

[34] X. Maldague, S. Marinetti and J. Couturier, "Applications of pulse phase thermography," *Review of Progress in Quantitative Nondestructive Evaluation*, Springer US, pp. 339-344 (1997)

[35] M. Ciniviz, E. Canlı, H. Köse, M. S. Salman and Ö Solmaz, "Ceramic Coating Applications and Research Fields for Internal Combustion Engines," *Ceramic Coating-Applications in Engineering,* InTech Open Access Publisher (2012)